UNIVERSITY OF TURKU

MXene and Ionic Liquid based Electrode Materials for Supercapacitors

Master's Thesis
Materials Chemistry
Aliisa Pakarinen

March 2023
Turku

Master of Science in Chemistry Thesis
Department of Chemistry, Faculty of Science
University of Turku

Subject: Chemistry
Programme: Master's Degree Programme in Materials Chemistry
Author: Aliisa Pakarinen
Title: MXene and Ionic Liquid based Electrode Materials for Supercapacitors
Supervisor: Ashwini Jadhav, Carita Kvarnström
Number of pages: 30 pages
Date: March 2023

MXenes are a new group of layered 2D materials that were discovered by Gogotsi et al. in 2011 and have gained lots of interest since. They have potential for many applications, showing excellent promise especially in electrical energy storage. They have mostly been studied for supercapacitors due to their 2D structure, good electrical conductivity, and hydrophilicity. Their capacitance values are already comparable with conventional carbon based supercapacitors, and as for that, MXenes have a possible role in future as an energy storage material once the performance reaches the required state in all the areas.

Ionic liquids have played an important role in electrochemical applications owing to their relatively low toxicity, low vapor pressure and a high stability. Herein we have used an environmentally friendly ionic liquid choline bis(trifluoromethylsulfonyl)imide to intercalate between the 2D MXene ($Ti_3C_2T_x$), which led to interlayer expansion between the sheets. The electrochemical performance of these composite materials was studied for supercapacitor applications.

The aim of this research was to enhance the electrochemical performance of $Ti_3C_2T_x$ by using ionic liquid as an intercalant to increase the interlayer spacing. $Ti_3C_2T_x$ was synthesized by etching aluminum from the corresponding MAX phase material (Ti_3AlC_2) by using LiF and HCl. The MXene – ionic liquid composite material was made by intercalating choline TFSI ionic liquid into the MXene powder in different ratios (2:1, 1:1, 1:2, 1:5 and 1:10). The composite materials were characterized using PXRD, UV-vis spectroscopy, TGA, FTIR and FESEM. Electrochemical performance was tested with cyclic voltammetry, galvanostatic charge – discharge and charge – discharge stability in H_2SO_4 electrolyte in a symmetric two electrode configuration.

Intercalation of ionic liquid into $Ti_3C_2T_x$ was successful for 2:1, 1:1 and 1:2 ratios as the interlayer spacing was increased. For 1:5 and 1:10 intercalation didn't expand the sheets. As the capacitance values for the composites remained low, further studies should be made to study the effect of surface chemistry on the electrochemical performance of the composite materials.

Keywords: intercalation, ionic liquid, MXene, supercapacitor, $Ti_3C_2T_x$

Table of contents

Terms used 4

1 Introduction 5

1.1 Supercapacitors 6

1.2 MXenes 9

1.3 MXenes as electrode materials 10

1.4 Ionic liquids 13

1.5 Intercalation 14

2 Experimental 16

2.1 Purpose of work 16

2.2 Chemicals 16

2.3 Synthesis of MXene and composites 17

2.4 Characterization 17

2.5 Fabrication of electrodes 18

2.6 Electrochemistry 18

2.7 Calculations 19

3 Results 20

3.1 Powder X-ray diffraction 20

3.2 Scanning electron microscopy 22

3.3 Thermogravimetric analysis 24

3.4 UV-vis spectroscopy 26

3.5 FT-IR 27

3.6 Conductivity 27

3.7 Electrochemistry 29

4 Future prospects 33

5 Conclusion 34

References 35

Terms used

2D	Two dimensional
AA	Alkyl ammonium
GCD	Galvanostatic charge-discharge measurement
CV	Cyclic voltammetry
c-LP	c-lattice parameter
DI	Deionized water
DMSO	Dimethyl sulfoxide
EDLC	Electric double layer capacitance
EV	Electric vehicle
FTIR	Fourier transfer infrared spectroscopy
ICE	Internal combustion engine
IL	Ionic liquid
PXRD	Powder X-Ray Diffraction
RTIL	Room-temperature ionic liquid
SEM	Scanning electron microscopy
TGA	Thermogravimetric analysis
XAS	X-ray absorption spectroscopy
XPS	X-ray photoelectron spectroscopy

1 Introduction

The shift from fossil fuel-based energy production to renewable energy sources is happening at an accelerating rate and while the change is necessary, it doesn't come without its challenges. For many renewable energy sources, the energy production is uneven and dependent on environmental factors. Solar power generates energy during sunny days and wind power reaches production peaks on windy days. As a result, renewable energy supply and demand don't always meet as weather conditions are uncontrollable. To harness the full potential of renewable energy sources, new energy storage methods are needed to support the grid and on the other hand provide alternatives for fossil fuels in applications that can't be plugged in all the time.[1] In many sectors decarbonization means electrification, and to achieve that, new efficient energy storage is required. For example, decarbonization of transport sectors relies on portable energy storage as vehicles can't be connected to the electrical network during drive. As cars are a necessary means of transport to many, reduction of emissions depends on portable energy storage technologies such as batteries, fuel cells, or supercapacitors.[2]

In 2020, road transportation contributed 11.9% of global greenhouse gases, from which around 60% was from passenger travel.[3] Strategy for reduction of these emissions consists of electrifying the transport sector by replacing internal combustion engine (ICE) vehicles with electric vehicles (EVs), increasing the role of green public transportation and shifting to more walkable and bike friendly infrastructure in cities.[4] While there are various approaches on how to carry out zero-emission vehicles, EVs are currently the most advanced and easiest technology to fit into the existing infrastructure and they already have an increasing market share in non-ICE vehicles[5]. Electrochemical energy storage is convenient solution for transportation due to its long cycle life, easily implemented infrastructure and state of the development compared to other technologies.[1,6]

Large scale energy storage applications are divided into mechanical, electrical, chemical, and electrochemical storage systems.[2] Batteries and supercapacitors are electrochemical energy storages that both have their own characteristics and applications. Batteries are the main source of energy in EVs, but they can benefit from pairing them with supercapacitors. Supercapacitors have also potential in stabilizing the power grid during uneven energy production. Development of electrode materials with higher energy and power density and longer cycle life is crucial to better take advantage of the theoretical possibilities that supercapacitors have to offer.

1.1 Supercapacitors

Supercapacitors are electrochemical energy storage devices, that are based on either electric double layer capacitance (EDLC) or pseudocapacitance. They fall in between conventional capacitors and batteries in terms of power density and energy density, as shown in Figure 1. Supercapacitors have high power density, which means they can be charged and discharged at a faster rate. They are suitable for applications requiring high rate capability such as balancing power supply in grid or hybrid electric vehicles.[7]

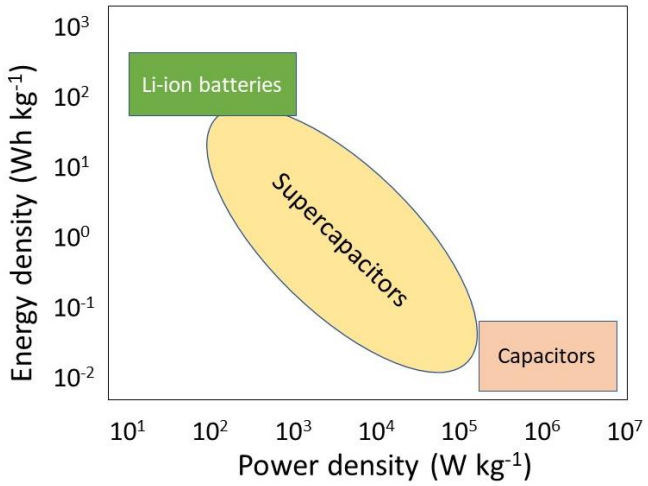

Figure 1 Ragone plot

Compared to batteries, supercapacitors have faster charging rate, but they come short in stored energy as they have low energy densities, which prevents their use as main energy storage devices in applications requiring a portable power source. However, due to lower power density, batteries suffer under sudden energy consumption, which happens during accelerating and braking. Supercapacitors could even out the strain of high peak energy usage if coupled with batteries, as they have high rate capability and withstand fast charging and discharging.[8] Another possible application in transportation for supercapacitors is electric busses in local public transport. While the energy density is weak in supercapacitors, providing only short range for one charge, the fast charging time makes them ideal for public transport busses, which have predetermined routes. By assembling high powered fast charging stations at bus stops, busses equipped with supercapacitors can charge at the stops during the route.

Supercapacitors are composed of two electrodes that are separated with a separator and an electrolyte (Figure 2). In conventional capacitors, the electrodes are separated with a dielectric, but the electrolyte in supercapacitors enables much smaller distance between the electrodes.

Thus, the energy density of supercapacitors is much higher although it still falls short from batteries. To increase the energy density of supercapacitor, a need for higher surface area electrodes and materials is evident. For example, in EDLC, capacitance depends on the specific surface area of the electrode that the electrolyte ions can access and form a capacitive layer on, and thus increasing the active surface area of the electrode then provides more space for the EDLC to form.[9]

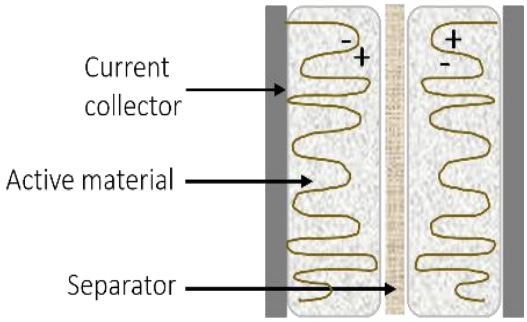

Figure 2 Supercapacitor configuration

Electric double layer capacitance is a non-faradic process, which means there's no charge transfer between the electrode and the electrolyte. The electrons or ions are accumulated on the electrode – electrolyte interface as potential is applied and charge is stored in the inner Helmholtz layer that forms on the electrode surface from the closest adsorpted species. Amount of electrical charge stored is limited by the surface area (effective active surface area) as following equation describes.[1]

$$C_{dl} = \frac{Q}{V} = \frac{\varepsilon_r \varepsilon_0 A}{d} \qquad (1)$$

In the equation, C_{dl} is the double layer capacitance, Q is charge that's transferred at potential V, ε_r and ε_0 are dielectric constants of the electrolyte and vacuum. A is the electrode surface area and d is the charge separation distance at the electrode.[1]

Current response for EDL type capacitors can be described as

$$I = \frac{dQ}{dt} = C_{dl}\frac{dV}{dt} \qquad (2)$$

where t is the discharge time. When the voltage change is linear with time ($V=V_0+ \nu t$, ν is scan rate) the relationship is described as

$$I = C_{dl}v \qquad (3)$$

Current correlates linearly with scan rate and in an ideal case, a cyclic voltammogram translates to a rectangular I-V plot. In galvanostatic charge-discharge (GCD) where the current is constant, the plot is triangular as the voltage increases and decreases at constant rate. These are the characteristics of EDLC in electrochemical measurements.[1]

Pseudocapacitance is a faradaic reaction. An electroactive species (ions) is electrosorpted on the electrode surface, where it undergoes a fast redox reaction with charge transfer. Pseudocapacitance occurs from faradaic processes that are divided into underpotential deposition (UDP), redox pseudocapacitance and intercalation pseudocapacitance.[10] In UDP monolayer of reduced metal ions forms on a metal surface to which a potential is applied. The resulting potential is less negative than the equilibrium of the metal ions. In redox pseudocapacitance electroactive ions are adsorpted on the electrode surface or the near surface region and undergo faradaic charge transfer reactions. Intercalation pseudocapacitance is based on faradaic processes that happen when intercalation of electroactive species into 2D material occurs. Unlike in battery electrodes, the intercalation doesn't involve crystallographic phase transformation. Each pseudocapacitance type takes place in different materials while still possessing similar thermodynamic traits.[1]

While ideal EDLC CV plot is an even rectangle, pseudocapacitive CV profile has redox peaks. GCD profile also have a slope instead of a triangle.[1] Despite the different mechanism in EDLC and pseudocapacitance, EDLC supercapacitors always have around 1-5 % pseudocapacitance and pseudocapacitors have around 5-10 % EDLC behaviour.[10]

The conventional electrode materials for supercapacitors are various carbon based materials for EDLC and transition metal oxides and conducting polymers for pseudocapacitors. Metal oxides provide better capacitance through pseudocapacitance compared to EDLC, but they suffer from low electric conductivity and electrochemical stability, which reduces their rate capability and cycle life.[11] Many approaches have been taken to tackle the problem, for example modifying the electrode morphology, particle size and developing hybrid materials. Discovery of new materials has accelerated the research, especially in 2D materials, such as graphene and even more recently discovered, MXenes. MXenes are a group of layered 2D material, which makes them suitable for intercalation of ions and furthermore a great media for intercalation/redox pseudocapacitance.

1.2 MXenes

MXenes are a growing group of ternary transition metal carbides, carbonitrides and nitrides with exceptional electric, mechanical, and optical properties and hydrophilic nature. The general formula of a MXene is $M_{n+1}X_nT_x$, where M is an early transition metal, X is carbon and/or nitrogen and T is surface termination species such as hydroxyl group, oxygen or fluorine and n=1, 2 or 3. They are generally synthesized from corresponding MAX phase by selectively etching out the A layer, which is group 13 or 14 element, usually aluminium, but synthesis methods for other compositions have been developed. MAX and corresponding MXene structures are shown in Figure 3. Due to the material's resemblance to graphene's morphology, it was named MXene.[12,13]

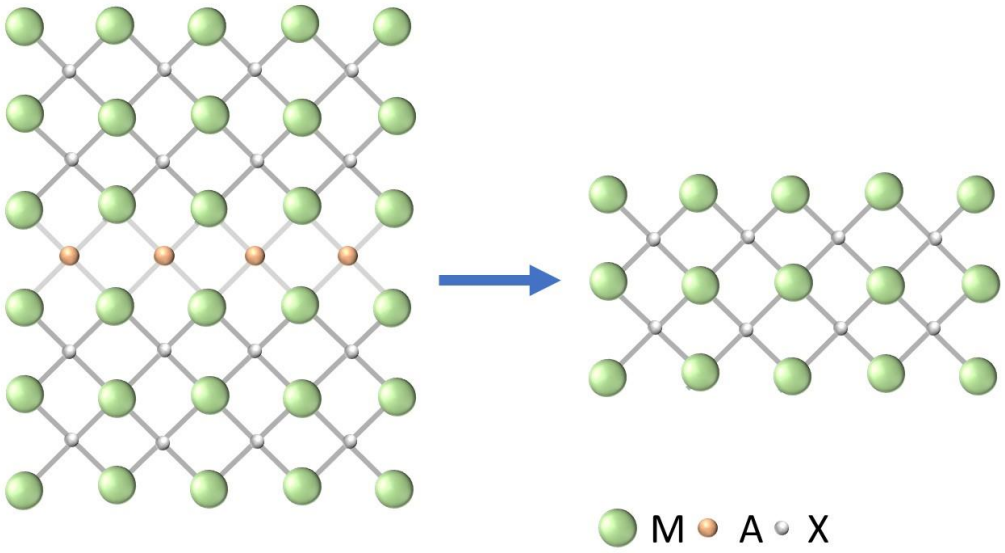

Figure 3 MAX and M_3X_2 MXene structure after etching

Removal of A from MAX phase is based on the difference in chemical reactivity of M – A and M – X bonds, former of which is weaker and can be broken by chemical etching with an acid. Initial synthesis was performed with HF, which produces 'accordion'-like multilayer structure with highly defined MXene layers. Those were then delaminated by intercalating some small molecules into the layers and sonicating them to obtain few layer MXene sheets.[14] In 2014 Gogotsi et al. managed to produce MXenes with another chemical etching method, which included the use of fluoride salt and hydrochloride.[15] Unlike with HF, which required an additional step for delaminating the layers, this new approach etched and delaminated MXene in single step. This along with safety reasons has made this method referred to as MILD method the most popular synthesis route in single layer MXene research.[6] In MILD method the highly

selective etching of A layer from the MAX phase is done by *in situ* formation of hydrofluoric acid by combining HCl and some fluoride salt such as LiF.[15]

To study the 2D properties of MXenes, they need to be delaminated. Compared to other layered materials, MXenes have strong interlayer interactions and intercalation has proven to be the most efficient delamination method. Intercalation can be done with various molecules but in MILD method, MXene is simultaneously intercalated with the cation from metal halide (Li^+) and water. Intercalation and mechanical vibration or sonication leads to single or few layered MXenes. Separate delamination step is required when MXene is etched with hydrofluoric acid as there's no ions or molecules to intercalate into the structure.[13]

While selective etching of MAX is the most common method for MXene synthesis, it is possible to synthesize them through other methods as well. The advantage of most of the other synthesis methods are that they enable the synthesis of certain MXenes that are not possible to produce with chemical etching and also offer a fluoride free etching process for more sustainable synthesis.[16] For example, molten salt synthesis can produce 2D transition metal nitrides[17] and MXenes from non-aluminium MAX phases[18] and electrochemical method was developed for fluoride free synthesis route[16]. In addition to environmental concerns, fluoride ions stay on the MXene as surface termination, affecting its properties. Preventing F-terminations through synthesis route is one option to modify MXenes for specific functionality.[16,19] Overall, etching method and conditions have major role in different structures and qualities that are obtained.

The first MXene Gogotsi et al. synthesised was $Ti_3C_2T_x$ from Ti_3AlC_2 MAX phase.[12] Ti_3AlC_2 showed most promise and was already widely studied material among MAX phase materials. $Ti_3C_2T_x$ is a thermally and electrochemically stable MXene, but many of its properties derive from its surface terminations. Ti_3AlC_2 belongs to group of over 150 different MAX phases[20], meaning there are theoretically as many possible MXenes also.[12] Some MXenes that have been synthesised include Ti_2C, Ta_4C_3, TiNbC and Ti_3CN_x, where $x<1$ but currently around different 40 MXene compositions have been reported in total.[21,22] The discovery of MXenes was significant as it introduced a completely new group of 2D materials, which there are only few despite their interesting properties and possibilities for various applications.[12]

1.3 MXenes as electrode materials

Electrode materials for supercapacitors need to have good conductivity and be chemically stable. Different carbon materials such as activated carbon, carbon nanotube, graphene and

graphene like 2D materials have been prominent in supercapacitor applications.[7] MXenes are an exceptional candidate as they provide high capacitance, long cycle life, as well as good rate capability. Factors that affect the capacitive performance of MXene based supercapacitors are its 2D structure, M and X composition, surface terminations, interlayer spacing and electrolyte.

One of the first attempts to use MXenes as supercapacitor electrodes was in 2013 by Lukatskaya et al. who prepared binder free $Ti_3C_2T_x$ filtrated paper electrodes via HF synthesis and achieved higher volumetric capacitances than previously had been for conventional carbon and graphene based EDLC supercapacitors.[23] Since then, MXenes have proven to be pseudocapacitive materials with high cyclic stability and high rate capability in aqueous and non-aqueous electrolytes. These properties are due the ion intercalation charge storage mechanism, which results in high gravimetric capacitance, and thus high volumetric capacitance. Good volumetric capacitance is an important feature when developing devices with high energy and power density. High power density and rate performance are characteristic for supercapacitors, and they are due to highly conductive electrodes.[6] This makes MXenes a fitting material for supercapacitor electrodes as they exhibit high metallic-like conductivity that is possible to modify by switching up the composition of M, X and the surface terminations.

Due to aqueous fluoride containing etching solution, –F, –OH and –O are the most common surface terminations in freshly synthesized MXenes. Surface terminations affect the electrochemical performance via changes in electronic conductivity, interlayer spacing and ion adsorption. While F-containing etchants are the most efficient ones and result in high quality MXene, –F terminations have a detrimental effect on the capacitive performance of MXenes. The detrimental effects of fluorine terminations include blocking of electrolyte ion transport[24], limitation of active redox sites by taking place from –OH and –O terminations and decrease in electronic conductivity.[25] It was discovered that thermal annealing removes –F terminations, which then increases the electrical conductivity.[25] Thus, methods for removal of –F terminations and development of effective fluoride-free etching methods is of great interest.

Understanding the charge storage mechanism in MXenes is important when developing and enhancing their electrochemical properties for energy storage applications. The storage mechanism in MXenes is not yet completely understood, but it is dependent on the electrolyte pH and charge carriers and it also differs between aqueous and non-aqueous electrolytes.[23,26,27] H_2SO_4 as an electrolyte provides high capacitance, good rate capability and long cycle life, which is the reason for its popular use as an electrolyte.[26] In H_2SO_4 the capacitance is

pseudocapacitive based in redox intercalation reactions, in which Ti of Ti_3C_2 changes oxidation state continuously upon charging and discharging. This is behaviour derives from the 2D structure of MXene, where active sites are accessed due to spontaneous ion intercalation and fast charge transfer is due to the conductive carbide layer.[26] In aqueous electrolyte, H_2O molecules also intercalate between layers and provide increased transport of H^+ ions, possibly via Grotthuss mechanism through a hydrogen bonding network.[28] The change in oxidation state is due to the bonding between electrolyte cations and surface terminations of the MXene. Surface terminations also affect the capacitive performance. –OH terminations have a positive effect by facilitating H_2O intercalation but excess –OH is detrimental for proton transport, as it disrupts the organization of intercalated molecules, limiting the power performance.[28] Thus, pseudocapacitive behaviour of MXene depends strongly on H^+ ion of the electrolyte and the surface chemistry of the material and can be developed further by changing these factors.[29]

Despite the high capacitances, aqueous electrolytes suffer from low energy densities due to water splitting at potentials higher than 1.23 V, and thus have limited potential range. This attracts the research of electrolytes with better electrochemical stability, such as ionic liquids and organic solvents. These electrolytes provide higher potential windows than aqueous electrolytes as they are more thermodynamically stable and aren't limited by decomposition at high potentials (above ~ 1 V). MXenes in ionic liquid based electrolytes are a safe and environmentally friendly alternative to aqueous and organic solvents with large electrochemical window, which provides a higher energy density for the device. In them, the storage is also based on intercalation of the cation, which causes volume change of the electrode as the ion swap places in charge/discharge process. Cations intercalate at negative potentials and swap with anion at positive potential.[30] Due to the large size of these ions and their slow mobility, MXenes can achieve only relatively low capacitances in ionic liquid -based electrolytes.

Intercalation or addition of spacers into the MXene layers is one method to increase the capacitance of MXene based supercapacitors. There are few approaches that've been applied and exhibited positive results, for example Liang et al. found out that pre-intercalation of $Ti_3C_2T_x$ with alkylammonium cations results in much higher capacitances in EMIM TFSI than pristine $Ti_3C_2T_x$ in EMIM TFSI, indicating that increased interlayer spacing allows the $EMIM^+$ to act as a charge carrier during the charging.[31] Addition of spacers prevents restacking of the sheets and increase the interlayer spacing, which gives better access to the active sites, thus increasing the capacitance.[32] Some of the spacers that've been studied include carbon nanotubes, hydrazine, CTAB via electrostatic intercalation, ion exchange or co-filtration of

such species. Intercalation as means to improve MXene's capacitive performance is further discussed in section 1.5.

1.4 Ionic liquids

Ionic liquids are salts in liquid state. They are made of ions, which makes them highly conductive and among other physical properties, attractive for various applications. Most salts turn liquid at some temperature, but room temperature ionic liquids, RTILs, are defined as liquid at ambient temperatures, making them useful in many fields of research and application. Besides their great ionic and electrical conductivity, they have high electrochemical stability and low vapor pressure.[33]

Most ionic liquids are also non-volatile and non-flammable due to the low vapor pressures. That makes them safer than the alternatives, and although they're not necessary less toxic than organic solvents, the low vapor pressure decreases the harmful exposure to them.[33] Flame retardancy is important property for materials in energy devices that require safe materials against accidental explosion and ignition. Ionic liquids are considered green solvents, making them an important topic in research to meet the standards for sustainable development and moving to greener technologies.[34]

Ionic liquids withstand high potentials up to 6 V providing a new electrochemically stable electrolytes for devices with higher energy density. Aqueous electrolytes and organic solvents are a major contributor of chemical waste while also providing lesser potential windows due to low thermodynamic stability (1.23 V for water and 2.7 V for acetonitrile).[34,35]

Due to their properties, ILs have become candidates as electrolytes in many electrochemical applications such as batteries and supercapacitors as they provide a safer option to organic solvents and larger potential windows than aqueous electrolytes. Other applications for RTILs are hydrogenation, polymerization, catalyst in organic reactions and as solvents in synthesis.[33] Some other groups of ionic liquids are chiral ionic liquids and task specific ionic liquids.[33]

Possibility to design endless combinations of ionic liquids by varying the anion and cation has made ionic liquids their own field of study as the properties can be tuned to be suitable for their needed application. The physical properties of ionic liquids depend on their complexity, bulkiness of ions, length of alkyl chains, nucleophilicity and correlation of ions [33] and anion-cation interactions[34] and hence are difficult to predict beforehand. Most studied ionic liquids are imidazolium-based ILs, in which cation consists of an imidazolium ring that has various

functional groups attached to it. Other common cations include ammonium, pyridinium thiazolium and phosphonium species among others. Some examples of anions are tetrafluoroborate, triflate and dicyanamide.[34]

Wang et al. implemented choline bis(trifluoromethylsulfonyl)imide (choline TFSI) as electrolyte in low temperature EDLC supercapacitors to overcome corrosivity issues in choline salt -based electrolytes.[36] Choline salts have shown great advantages as EDLC electrolytes due to being eco-friendly, cost-efficient, and durable in low temperatures but halides that were used in those studies as counter ions were corrosive for stainless steel current collectors. This led to the combining of eco-friendly choline$^+$ and stable and non-corrosive TFSI$^-$ for the electrolyte. Due to the hydrophobicity of TFSI$^-$, choline TFSI has a very low water solubility. Wang et al. used choline TFSI in aqueous electrolyte, and to overcome the low water solubility they used methanol and isopropanol as cosolvent.[36] Despite its advantages, choline TFSI hasn't been widely used for electrochemical applications.

1.5 Intercalation

MXenes are capable to accommodate various intercalants in their structure. Intercalation and level of delamination of the sheets is mainly studied by detecting the c-lattice parameters (c-LP) and d-spacing from X-ray diffraction data, as intercalants increase c-LP by breaking and weakening van der Waals bonds between the layers.[37,38] During etching, impurities, oxidation and chemical degradation cause decline in MXene's activity, physical properties and performance. Intercalation of any additives has been detected to improve MXenes' performance and enhance their stability and quality by tuning kinetics and thermodynamics and modulating their electronic properties.[38]

Delamination and intercalation are required steps to achieve few or single layer MXenes from MAX phase precursors and it can be done simultaneously or in sequential steps. Effective intercalants are categorized into molecules, cations and organic bases.[38] Typical cations used for intercalation are ones like NH^{3+}, K^+, Li^+, H^+ etc.,[38] but to further increase the layer spacing, large polyatomic cations are proven to be efficient intercalants as well.[31,39,40]

Ghidiu et al. used alkylammonium salts $[(CH_3)_3NR]^+$, where R represents CH_3, C_6H_{13}, $C_{10}H_{21}$, $C_{12}H_{25}$ or $C_{16}H_{33}$, to study how size of the intercalating cation affects the spacing by varying the length of alkyl group.[40] Liang et al. did something similar by pre-intercalating MXenes with alkyl ammonium cations (AA) of varying length to use in room temperature ionic liquid.[31] Both

discovered that increasing the length of alkyl group increased the interlayer spacing of the MXene layers as the cation replaced Li^+/Na^+ ions used in etching by cation exchange mechanism.[31,40] Liang et al. were interested in enhancing the electrochemical properties in organic and RTIL electrolytes as the larger ions in those cause hindrance in intercalation of the cation. They achieved higher specific capacitances in EmimTFSI for $Ti_3C_2T_x$ that were pre-intercalated with AA-cation with longer alkyl chain than pristine $Ti_3C_2T_x$.[31]

As MXenes can accommodate cations in their sheet structure, the idea to use ionic liquids to delaminate the material was considered. Pre-intercalation of MXenes with ionic liquids is a new, less researched concept. Previously Zheng et al. have studied ionic liquid pre-intercalated MXenes for ionogel-based micro-supercapacitors. They used $EmimBF_4$ as intercalated IL as well as for the electrolyte and achieved one of the highest reported volumetric energy densities.[41] They also noticed high electrical conductivity and an enhanced ion transport network as a result from larger interspacing from the intercalated ionic liquid, which provided more space for the electrolyte ions to reach active sites within the material.[41] Figure 4 shows the procedure for MXene synthesis and ionic liquid intercalation.

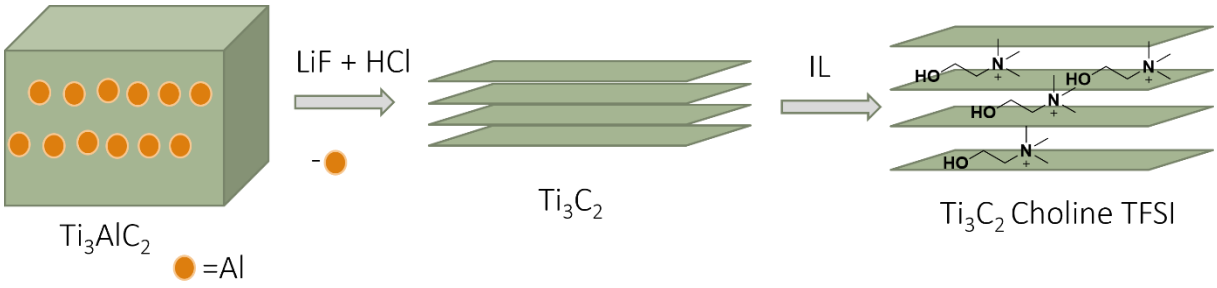

Figure 4 MXene synthesis and intercalation of ionic liquid

2 Experimental

2.1 Purpose of work

Intercalation of small molecules has been found to increase the interlayer spacing of MXenes, which again has positive effect on electrochemical performance of MXenes. Ionic liquids are an intriguing group of non-aqueous electrolytes that have potential in electrochemical energy storage systems such as supercapacitors. Purpose of this work was to study how intercalation of ionic liquid into MXene would affect its electrochemical properties and suitability for MXene based electrodes for supercapacitors.

As this subject is not yet studied extensively, in this project the chosen materials were $Ti_3C_2T_x$, as it's well known and stable MXene and Choline bis(trifluoromethylsulfonyl)imide (choline TFSI) as it's eco-friendly and affordable ionic liquid. Choline TFSI was intercalated into MXene ($Ti_3C_2T_x$), which was synthesised in LiF/HCl etching solution for 48 hours and the electrochemical performance of the electrodes was studied by cyclic voltammetry (CV) and galvanostatic charge-discharge (GCD). Intercalation was done in five different ratios to get an understanding on how different amounts of intercalant affects the properties of $Ti_3C_2T_x$ and in attempt to increase its performance further. Electrolyte that was chosen was H_2SO_4 as it currently provides the best electrochemical performance.

2.2 Chemicals

Hydrochloric acid (37%) was purchased from VWR, lithium fluoride (98.5%) from Alfa Aesar and Ti_3AlC_2 from Carbon Ukraine. Choline bis(trifluoromethylsulfonyl)imide (Figure 5) was purchased from IoLiTec-Ionic Liquids Technologies GmbH. Acetonitrile (≥99.9%) and Nafion® perfluorinated resin solution 5 wt% was purchased Sigma-Aldrich. Carbon black is from Asbury carbons and graphite foil (0.5 mm thick, 99.8% (metals basis)) is from Thermo Scientific. Sulfuric acid solution, 2.5 M (H_2SO_4) was purchased from Fluka Analytics and NMP (1-Methyl-2-pyrrolidinone) from TCI.

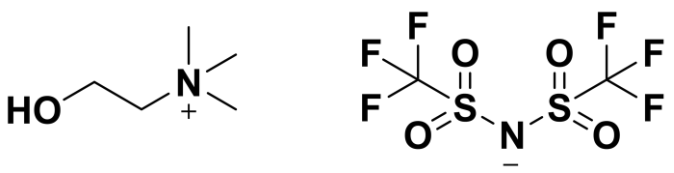

Figure 5 Molecular structure of choline TFSI

2.3 Synthesis of MXene and composites

$Ti_3C_2T_x$ was synthesised by etching Ti_3AlC_2 with LiF/HCL solution. 1g of LiF was dissolved in 20 ml of 6 M HCl and it was stirred at 500 rpm in a plastic bottle. After 5 minutes, 1 g of crushed Ti_3AlC_2 powder was added slowly over a time approximately 5 minutes, to avoid heat generation. The reaction was left to proceed for 48 hours under magnetic stirring at 45 °C. Once the solution was cooled to room temperature, it was transferred to centrifuge tubes and distilled water was added to around 40 ml. First centrifuge cycle was 10 minutes at 3500 rpm, after which the pH of supernatant was checked with pH paper and then disposed. This step was repeated until the supernatant was neutral, which required seven cycles. Next 10 ml of distilled water was added to the mixture and the product was filtered with filter paper in a vacuum filter and then let to dry in a vacuum desiccator at room temperature.

Intercalation of ionic liquid (IL) between dry $Ti_3C_2T_x$ sheets was carried out in five ratios that were 2:1, 1:1, 1:2, 1:5 and 1:10 (MXene to IL). The samples are referred by their intercalation ratio from now on. Choline TFSI was dried in a vacuum oven at 80 °C for 2 hours to remove water before intercalation. Appropriate amounts of $Ti_3C_2T_x$ and choline TFSI were mixed in 4 ml of acetonitrile for 24 hours under magnetic stirring. Then the mixture was washed in centrifuge and dried in a vacuum desiccator at room temperature. Samples were stored in a desiccator at room temperature.

2.4 Characterization

Powder X-ray diffraction (PXRD) measurements were obtained with PANanalytical Aeris diffractometer using Cu Kα radiation source (λ=1.5406 Å). Thermogravimetric analysis (TGA) was performed with TA Instruments Q600 SDT from 20 °C to 1000 °C in nitrogen atmosphere and with 10°C/min flow rate. Scanning electron microscope (SEM) images were obtained with Thermo Scientific Apreo SEM instrument. UV-vis spectra were measured with Agilent Cary 60 UV-vis spectrometer from 200 nm to 1000 nm colloidal solution in distilled water. FTIR spectra of $Ti_3C_2T_x$, the composites and choline TFSI was collected using Bruker FTIR instrument from 400 to 4000 cm^{-1}. Electrochemical measurements were performed with Iviumstat potentiostat in a symmetrical two-electrode cell using 0.1 M H_2SO_4 electrolyte. The system is pictured in Figure 6. Conductivity of materials was measured from pressed MXene pellets using Keithley 2460 source meter.

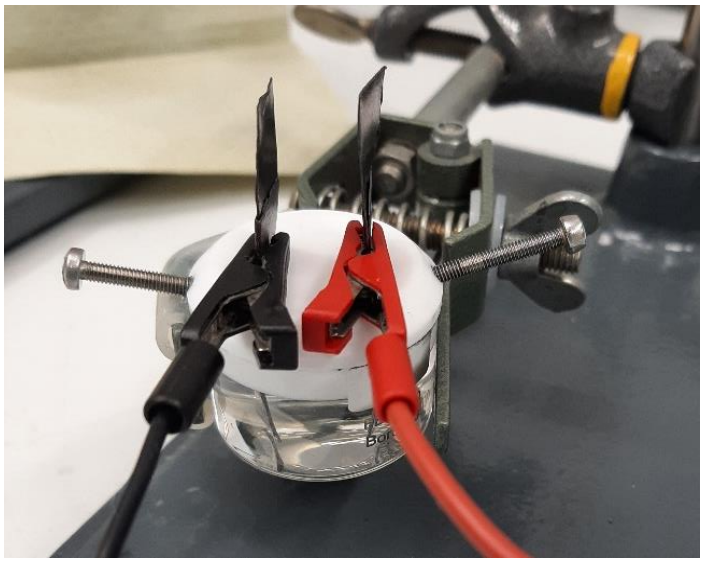

Figure 6 The cell used in electrochemical measurements

2.5 Fabrication of electrodes

Electrodes were fabricated on grafoil strips by mixing active material ($Ti_3C_2T_x$ composite and/or conducting carbon) with the binder (Nafion) and solvent (NMP) and drop casting the mixture on 1.0 cm^2 area with 2 mg/cm^2 mass loading. Electrodes were dried in an oven at 120 °C for minimum of 4 hours. Materials were tested with and without conducting carbon.

2.6 Electrochemistry

Electrochemical measurements were done using IviumStat potentiostat in a symmetrical two-electrode cell with 0.1 M sulfuric acid as electrolyte on potential window from -0.5 to 0.5 V. Electrolyte was purged with nitrogen gas for 10 minutes before measurements and electrodes were saturated before each measurement by carrying out 15 CV cycles at 50 mV/s. CV was measured with five scan rates: 5, 10, 50, 100 and 200 mV/s from -0.5 to 0.5 V. Each scan rate was cycled four times and the last scan was used for calculations and plotting. The used current range was 10 mA and potential step 0.1 V. Charge-discharge measurements were done immediately after CV measurements in same electrolyte with the same potential window. Currents densities used were 0.2, 0.4, 0.8, 2 and 6 mA/cm^2 and each measurement was repeated four times.

2.7 Calculations

Resistance values are listed in Table 2 and they're calculated from conductivity measurements as follows:

$$R = \frac{V}{I} = \frac{1}{slope} \quad (4)$$

where V is potential, and I is current. Capacitance from 2-electrode CVs is calculated by integrating the discharge cycle of the CV with following equation.

$$C = \int_{V_1}^{V_2} \frac{I(V)dV}{Vx\frac{dV}{dt}} \quad (5)$$

$$\int_{V_1}^{V_2} I(V)dV \quad (6)$$

$$C_A = \frac{C_{electrode}}{A} \quad (7)$$

$$C_G = \frac{C_{electrode}}{m} \quad (8)$$

C_A is the areal capacitance and C_G is the gravimetric capacitance of a material. A is area of the electrode, and *m* is the mass loading of active material. Capacitance from GCDs is calculated with equation 9 from the discharging sequence of the measurement. Because the electro-chemical cell was a 2-electrode system, the capacitance is multiplied by two. C_A and C_G are calculated from C_{cell} in the same way as in equations 7 and 8.

$$C_{cell} = \frac{2 \times I\Delta t}{\Delta V} \quad (9)$$

For MXene, d-spacing consists of one MXene sheet and one interlayer spacing. c-lattice parameter is twice the d-spacing, so it's two MXene sheets and two interlayer spacings. d-spacing of each MXene sample are calculated from PXRD data with following equations. c-LP and interlayer spacing is obtained from those values, which are reported in Table 1 along with positions of (002) peaks.

Equation for calculating d-spacing between sheets is

$$2dsin\theta = \lambda \quad (10)$$

$$d_{nkl} = \frac{\lambda}{2sin\theta} \quad (11)$$

where λ is the wavelength if the X-ray and θ is half of the 2 theta value. Interlayer spacing for composite is obtained by subtracting the d-spacing of dry $Ti_3C_2T_x$ from the d-spacing of the composite.

3 Results

3.1 Powder X-ray diffraction

PXRD is one of the most useful characterization methods to verify the complete etching of MAX phase and the formation of MXene. Ti_3AlC_2 exhibits all the typical peaks corresponding to $p6_3/mmc$ crystal structure. In the case of $Ti_3C_2T_x$, the higher order peaks are absent and (00l) peaks are shifted to a lower theta and broadened.[12] By observing the disappearance of the peaks corresponding to Ti_3AlC_2 and shifting of (002) peak MXene is confirmed as a synthesis product. PXRD data also gives information on the crystallite size, layer thickness and interlayer spacing of MXene, which are used to study intercalation.[37]

$Ti_3C_2T_x$ was synthesised by reacting Ti_3AlC_2 in LiF/HCl for 24 hours and 48 hours to monitor the time required for complete etching. PXRD for Ti_3AlC_2 and $Ti_3C_2T_x$ with 24 hours reaction time and $Ti_3C_2T_x$ with 48 hour reaction times is shown in Figure 7a. For $Ti_3C_2T_x$ -24h (002) peak corresponding to the MAX phase at 9.5 2 theta is present as well as the peak corresponding to aluminium at 38.8 2 theta indicating incomplete etching. For $Ti_3C_2T_x$ -48h these peaks are absent, confirming a successful reaction to MXene with only minor impurities from starting material.

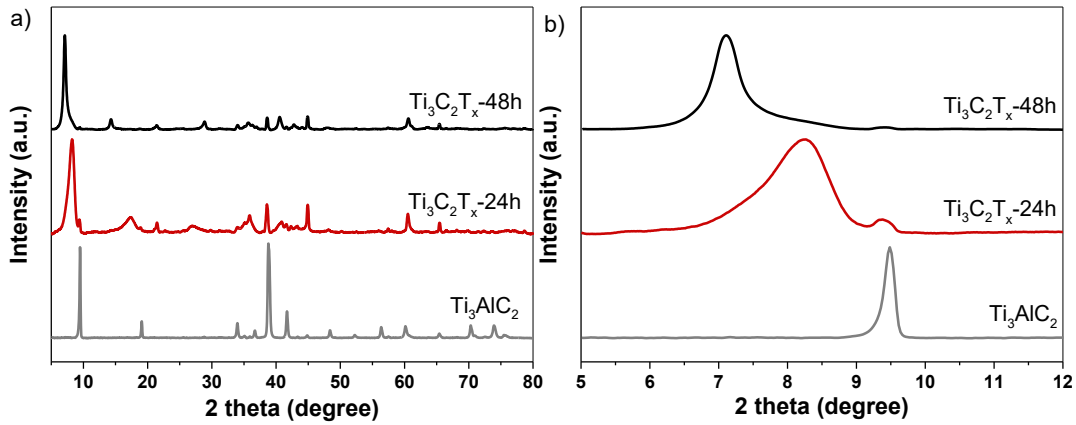

Figure 7 a) Ti_3AlC_2, and $Ti_3C_2T_x$ with 24 hours and 48 hours reaction time b) 002 peak of MAX and synthesised MXene

Once etching was deemed successful, the resulting MXene was intercalated with ionic liquid in different ratios and the PXRD was obtained for the MXene/IL composites to observe the effect on interlayer spacing. Intercalation was first done in 2:1, 1:1 and 1:2 ratios and after promising results, continued with 1:5 and 1:10 ratios.

Intercalation of IL also shifts the (002) peak as the MXene sheets expand. Figure 8a shows PXRD spectra for $Ti_3C_2T_x$ and the composites and Figure 8b shows the corresponding change in the interlayer spacing. The position of (002) peak, c-lattice parameters and d-spacing of each sample are presented in Table 1.

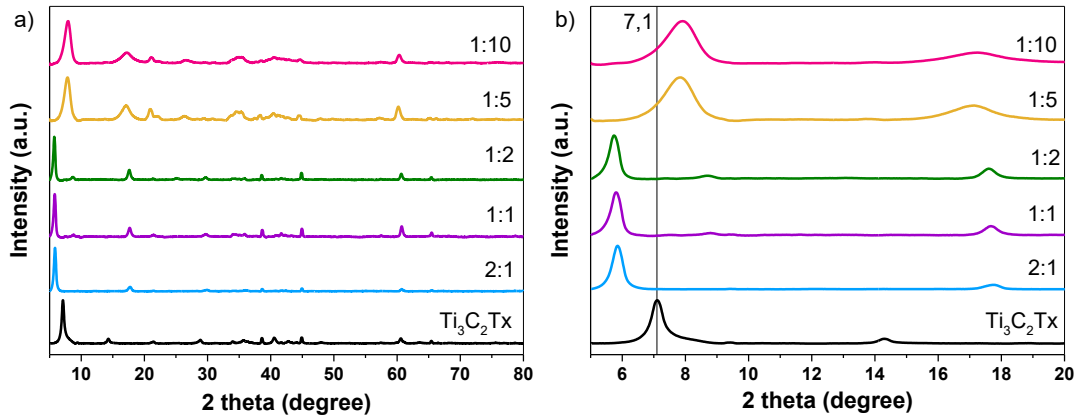

Figure 8 a) PXRD for $Ti_3C_2T_x$ and the intercalated materials b) positions of (002) peaks

Table 1 Position of (002) peaks, c-lattice parameters, d-spacing and interlayer spacings calculated from PXRD data for $Ti_3C_2T_x$ and ionic liquid composites

	(002) (2θ)	**c-lattice parameter (Å)**	**d-spacing (Å)**	**Interlayer spacing (Å)**
$Ti_3C_2T_x$	7.1	24.790	12.395	-
2:1	5.8	30.088	15.044	2.649
1:1	5.8	30.242	15.121	2.726
1:2	5.7	30.609	15.305	2.909
1:5	7.9	22.345	11.172	
1:10	7.9	22.450	11.225	

A shift in the (002) peak to a lower angle indicates expansion of MXene due to intercalation of ionic liquid into the sheets. Multiple studies made on intercalation of MXenes concluded that adding small molecules such as H_2O, dimethyl sulfoxide (DMSO) and alkylammonium cations into the structure enlarges the interlayer spacing to a certain degree.[31,40,42] With choline TFSI as the intercalant, this was observed for 2:1, 1:1 and 1:2 ratios.

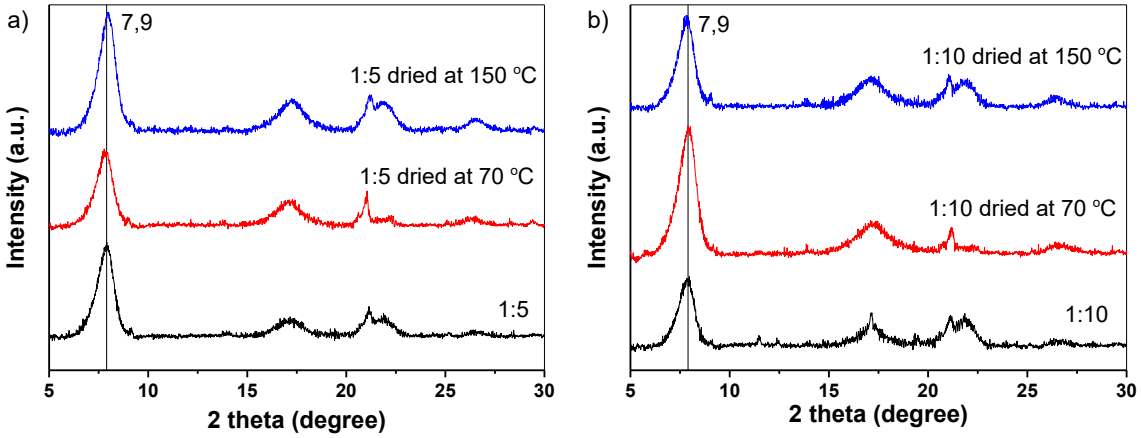

Figure 9 a) PXRD of 1:5 dried at room temperature (black), at 70 ºC (red) and at 150 ºC (blue) b) 1:10 dried at room temperature (black), at 70 ºC (red) and at 150 ºC (blue)

As the smaller ratioed samples showed promising results, it was expected that increasing the IL content to 1:5 and 1:10 would increase the interlayer spacing even more. However, for 1:5 and 1:10 the effect was opposite and the spacing grew smaller than it was in pristine $Ti_3C_2T_x$. Similar results were not found from the literature survey for other intercalants so the reason for this behaviour remains unclear. d-spacing of $Ti_3C_2T_x$ has been observed to grow much higher than reported here with increasing cation size. Zhou et al. mention in their article that freshly made MXene has higher (002) peak than MXene that's been dried for 168 hours in either room temperature, in vacuum or in oven owing to departure of water or other solvent from the structure.[43] Few tests were made to further study whether high temperatures would affect the interlayer spacing. Samples were put in vacuum oven at 70 ˚C and 150 ˚C overnight but as can be seen from Figure 9, there's no major changes in the PXRD pattern, implying that no further removal of water of other intercalants take place. A possible explanation for this result could be in hygroscopic nature of ionic liquid as excess ionic liquid could remove water from the interlayer spaces resulting in tight packing of MXene sheets. Further studies are needed to confirm this theory.

3.2 Scanning electron microscopy

FESEM was used to visualize the morphology of MXene flakes. Figure 10 shows SEM images of $Ti_3C_2T_x$ and the intercalated samples. Typically, MXenes are recognized from the highly separated 'accordion'-like structure, which is obtained when etching is done with hydrofluoric acid. 'Accordion'-like structure is result from gas production, most likely H_2, during intense HF synthesis, which expands the layers as is seen in SEM. Lower acid concentration and non-

HF synthesis such as LiF/HCl produces less prominent ‘accordion’-like structure due to weaker production of H_2[12,44]. The as synthesised particles are denser and look more closer to MAX phase, however, the morphology isn’t the only indication of quality of the produced MXene or the quantity of separation, which is elucidated from PXRD[13].

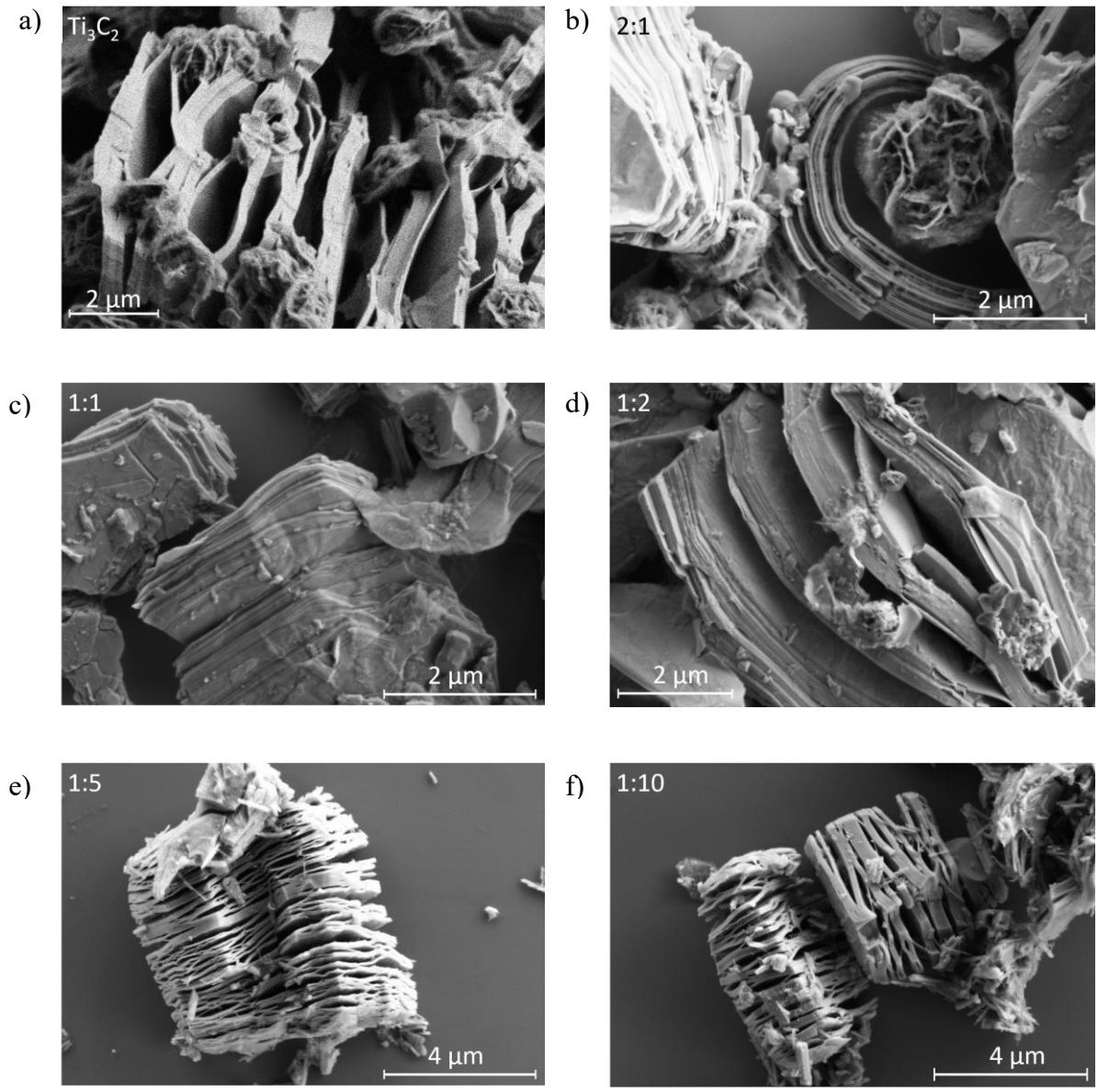

Figure 10 SEM images of $Ti_3C_2T_x$ and ionic liquid intercalated composites

Here LiF/HCl synthesised $Ti_3C_2T_x$ shows some visibly separated layers in Figure 10a. Intercalation expands MXene layers further which is seen in PXRD but looks less separated in SEM. Denser packing of the 2:1, 1:1 and 1:2 intercalated samples could be due to the intercalated species in between the layers.[13]

Although intercalation expands the layers, there's unexpected variation between the ionic liquid intercalated samples as has been seen from the PXRD. Samples in 2:1, 1:1 and 1:2 ratios have denser packing as expected but 1:5 and 1:10 intercalated samples have decreased interlayered spacing with more 'accordion'-like structure in SEM. The more separated layers in the SEM images for 1:5 and 1:10 samples support the conclusion that the ionic liquid wasn't intercalated in the first place, resulting in low interlayer spacing.

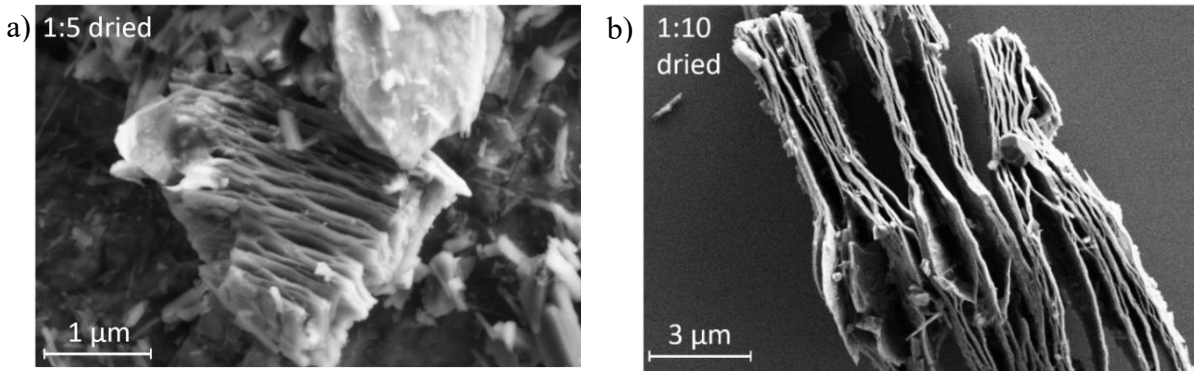

Figure 11 SEM images of a) 1:5 and b) 1:10 intercalated Ti_3C_2 that have been dried in oven at 150 °C overnight

SEM was obtained also from the dried 1:5 and 1:10 samples to see how the drying affected the morphology (Figure 11). Dried samples have well separated morphology in SEM and the drying doesn't seem to have much effect as was also detected with PXRD. Interlayer spacing is mostly contribution of intercalated water or other molecules, $choline^+$ in this instance.

3.3 Thermogravimetric analysis

TGA is used to study the thermal stability of MXenes. In this case it also acts as a confirmation that each sample with different intercalation ratios contain different amounts of ionic liquid within the material. Typically, TGA is used with gas analysis to detect the decomposition products like CO, which indicates decomposition of titanium carbide into cubic carbon in inert atmosphere. Reactive forms of oxygen are generated during heating, which leads to oxidation even if the atmosphere is oxygen-free. Phase transformation of $Ti_3C_2T_x$ takes place at critical temperature, which depends on the etching method and etchant concentration but is around 750 – 900 °C. Below that critical point, thermal annealing causes transformations in surface terminations and decomposition of functional groups. Thermal stability is affected by the surface terminations and defects in MXene structure, the composition of which depend on the etching conditions.[45] In this work, no gas analysis was done, but the results match those reported in literature.[37]

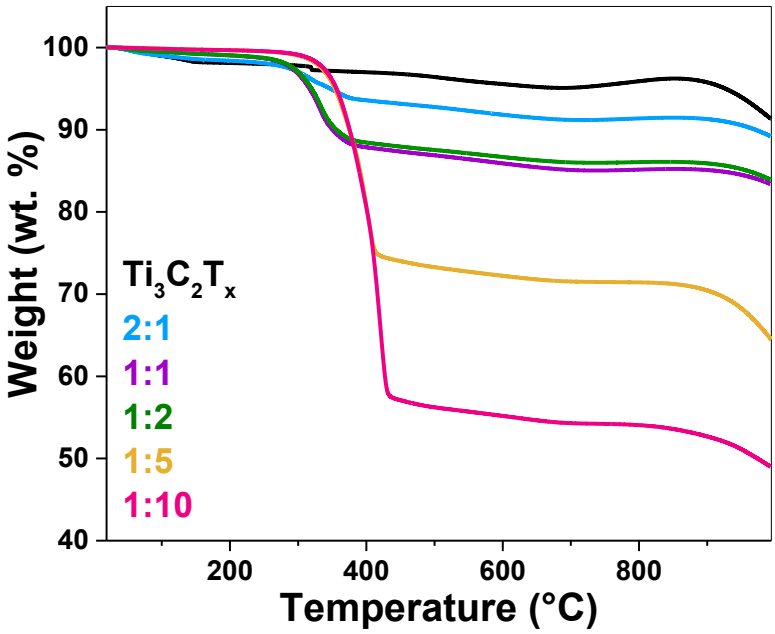

Figure 12 TGA graphs for all the samples

TGA graphs are shown in Figure 12. Most prominent weight loss happens around 330 ˚C, where the ionic liquid is decomposed. The weight loss is different for each sample, confirming that for each MXenes/IL ratio, there's different amounts of ionic liquid present in the sample, as the weight loss correlates with the increasing amount of ionic liquid. In $Ti_3C_2T_x$ graph (black), there's no decomposition at 330 ˚C while the sample with 1:10 ratio (pink) 40 % wt loss is observed. The weight loss from decomposition of choline TFSI correlates with the IL to MXene ratio on the samples, only exception being 1:1 (purple) and 1:2 (green) ratios, where there's no notable difference is observed. $Ti_3C_2T_x$ is stable until 800 ˚C. For the composites, the weight of the sample plateaus at 800 ˚C until 860 ˚C, where $Ti_3C_2T_x$ starts decomposing. The loss around 100 ˚C is attributed to water that's left from washing process.

Critical temperature value for any material's decomposition is suggestive and varies depending on experimental conditions such as heating rate and sample quantity. Most ionic liquids decompose below 400 ˚C,[46] and for multiple choline based ionic liquids decomposition starts around 200 ˚C (choline TFSI not included)[47]. The starting temperature for decomposition of choline TFSI is at around 250 ˚C, which is relatively close to those in literature for choline based and other ionic liquids when experimental set up differences are taken into account. Here choline TFSI was also intercalated into MXene, which affects the starting temperature for

decomposition. Higher quantity of ionic liquid in 1:10 correlates to the higher starting temperature in that sample.

3.4 UV-vis spectroscopy

As usual for nanoscale materials, MXenes have unusual optical properties. UV-vis spectroscopy is a simple way to characterize MXene – light interactions from thin films or colloidal suspensions and to detect the quality of synthesized MXene as well as confirm the synthesis product. Here UV-vis absorption was measured from suspensions of $Ti_3C_2T_x$ and $Ti_3C_2T_x$ /IL composites in DI water and the results are presented in Figure 13. $Ti_3C_2T_x$ has a distinct peak around 780 nm, which is from plasmon resonance/transverse plasmon mode. The green colour of diluted aqueous solutions of $Ti_3C_2T_x$ is due to this plasmon resonance.

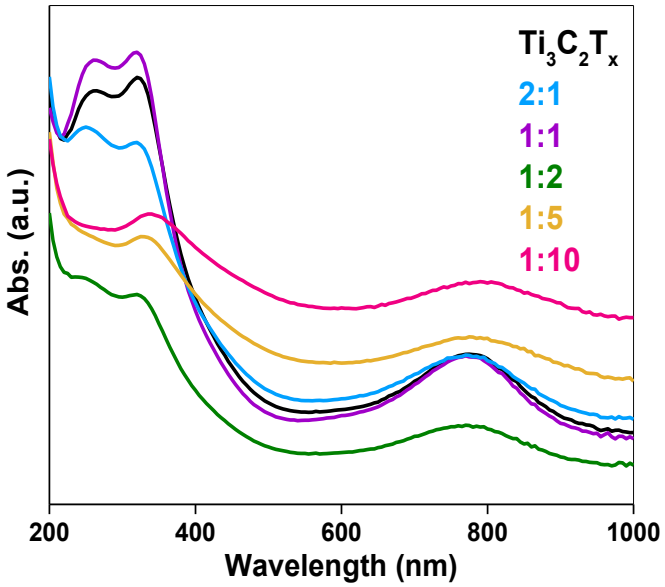

Figure 13 UV-vis graph of the samples

Plasmon resonance peak is present in all the samples, but as the ratio of ionic liquid increases, the contribution of choline TFSI in the spectra is more intense. The higher amount of intercalated choline TFSI weakens the absorption at 780 nm as well as the peaks around 300 nm. The 780 nm peak for 1:5 and 1:10 ratios is broader and less intense than for $Ti_3C_2T_x$ and 2:1, 1:1 and 1:2. 260 nm peak decreases with increasing IL ratio and 320 nm peak for 1:5 and 1:10 has minor shift to the right to 335 nm and 340 nm. The shift could be due to surface oxidation during storage of the material, as TiO_2 has an absorption at around 330 nm, but this should be confirmed in further experiments. These results indicate significant deviations in the

properties of 1:5 and 1:10 samples as is also observed from the all the analysis thus far. Differences in the overall absorption intensities of the samples is due to differences in the solution, as different ratios also affected the UV-vis measurements.

3.5 FT-IR

FT-IR measurements were performed to confirm the presence of choline TFSI in the samples and the spectra are presented in Figure 14. $Ti_3C_2T_x$ peaks would correspond to its surface terminations such as Ti – O stretching vibration at 550 cm^{-1} or C – O stretching vibration at 1060 cm^{-1} and the peaks for choline TFSI should be present in the composites' spectra, but it was difficult to obtain decent spectra due to the highly absorbing and static nature of MXenes.[43]

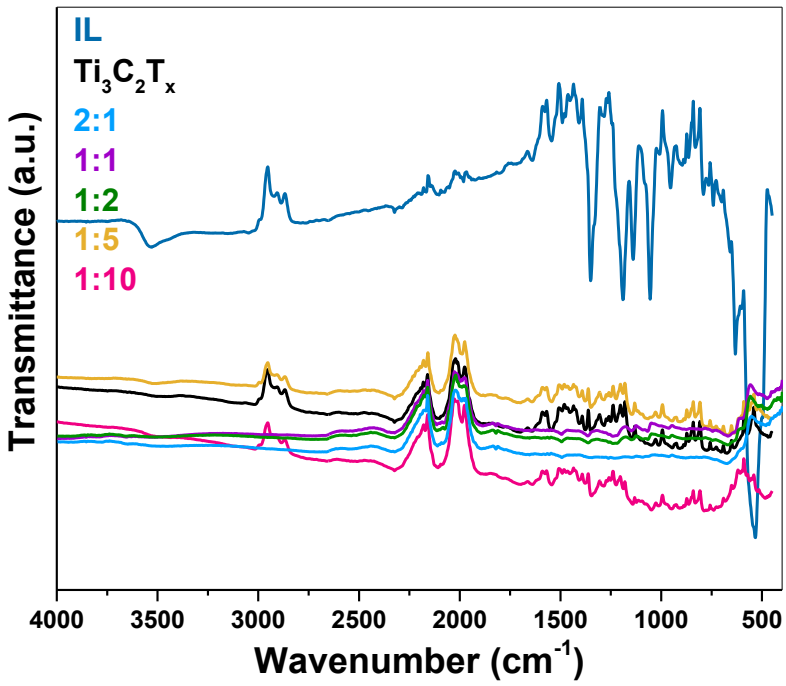

Figure 14 FTIR spectra of IL, $Ti_3C_2T_x$ and MXene composites

3.6 Conductivity

Resistance of the samples were measured with a linear 4-point probe and the results are shown in Figure 15. The resistances for $Ti_3C_2T_x$ and 2:1, 1:1, 1.2 and 1:5 composites are presented in Table 2. 1:10 was too soft due to the IL, so the pellets were not possible to make.

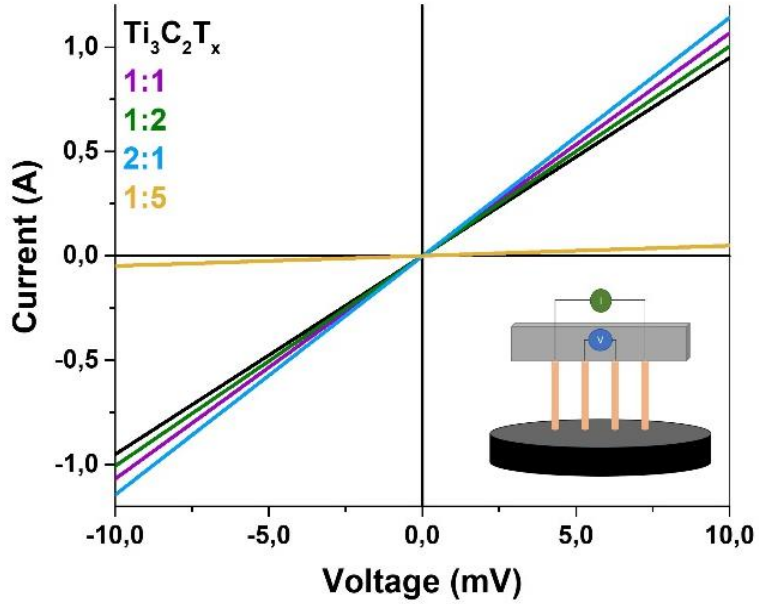

Figure 15 Conductivity measurements

$Ti_3C_2T_x$, 2:1, 1:1 and 1:2 have relatively low resistance around 10 mΩ in the same scale while 1:5 has much higher resistance at 206 mΩ. Resistance is inversely proportional to conductivity so based on the resistances, 1:5 has low conductivity compared to samples with lower ratios of IL. This correlates with capacitance results as a conductivity of a material is related to its capacitive properties. Lower conductivity of higher IL ratio could be due to less MXene and IL preventing interfacial contact between the fewer flakes, which again affects the capacitance. Resistance in other samples rises slightly with increasing IL concentration, but it doesn't seem to have major impact on capacitance and the difference is only milliohms. It's also been reported before, that intercalating organic compounds into MXene increases their resistivities by 1 to 2 magnitudes.[14]

Table 2 Resistances measured with Keithley 2460 source meter

	Resistance (*mΩ*)
$Ti_3C_2T_x$	10.5
2:1	8.8
1:1	9.4
1:2	10.0
1:5	206

3.7 Electrochemistry

Electrochemical performance of the materials was tested with and without conducting carbon. Figure 16a shows CV for electrode with conducting carbon with ~90 wt% of $Ti_3C_2T_x$ as active material, ~5 wt% of conducting carbon and ~5 wt% of Nafion as a binder. Figure 16b and c show CV and GCD respectively for electrode without conducting carbon, consisting of ~95 wt% of $Ti_3C_2T_x$ as active material and ~5 wt% Nafion as a binder. The test was performed to compare whether carbon in the electrode significantly increases the performance and should be included in the electrode configuration that would be used in the later measurements. For this, only CVs were measured, so capacitance values were calculated from CVs at 2 mV/s scan rate while for other samples results are reported from the discharge sequence of GCD measurements at 0.2 mA/cm^2. The capacitance values are listed in Table 3. Areal capacitance (C_a) for carbon containing electrode was 212 mF/cm^2 and for the one without carbon the value was 205 mF/cm^2. As similar values were achieved with both electrode configurations, experiments were continued without carbon.

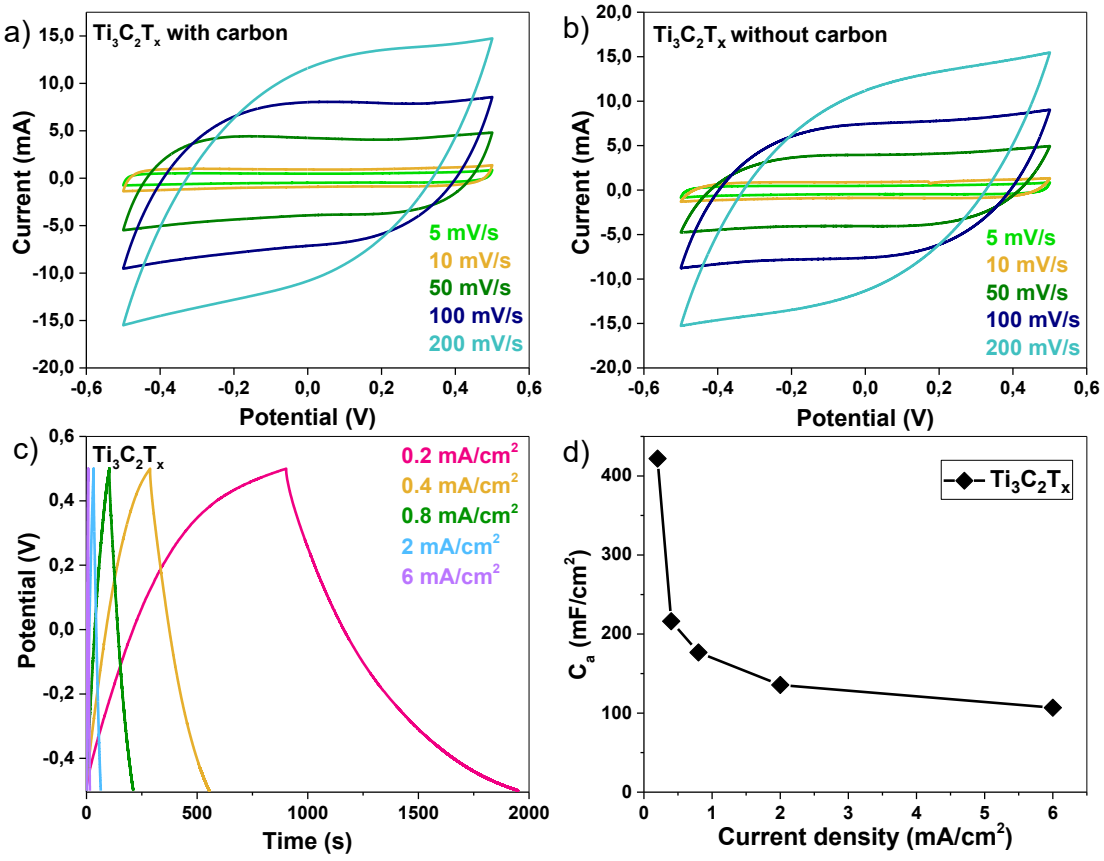

Figure 16 a) CV of $Ti_3C_2T_x$ with conducting carbon b) CV of $Ti_3C_2T_x$ without conducting carbon c) GCD of $Ti_3C_2T_x$ without conducting carbon and d) capacitances of $Ti_3C_2T_x$ without conducting carbon

Figure 17 shows CVs, GCDs and specific capacitances for samples 2:1, 1:1 and 2:1. Based on plots, the MXene/IL electrodes have EDLC type capacitance as the shape of the CVs are rectangular without redox peaks and GCDs have even triangular shape. Usually MXenes are pseudocapacitive materials in acidic aqueous electrolytes such as 1 M H_2SO_4 due H^+ intercalation, which results in high capacitances.[26] EDLC type capacitance is dominating in neutral and basic aqueous electrolytes.[48] However, there are reports of EDLC type capacitance in H_2SO_4, which may be due to the two electrode systems such as used here or the increased interlayer spacing.[49] Higher concentration of H_2SO_4 electrolyte corresponds to higher capacitance due to higher conductivity of the electrolyte[50], so the capacitive performance is good despite concentration of H_2SO_4 electrolyte being only 0.1 M.

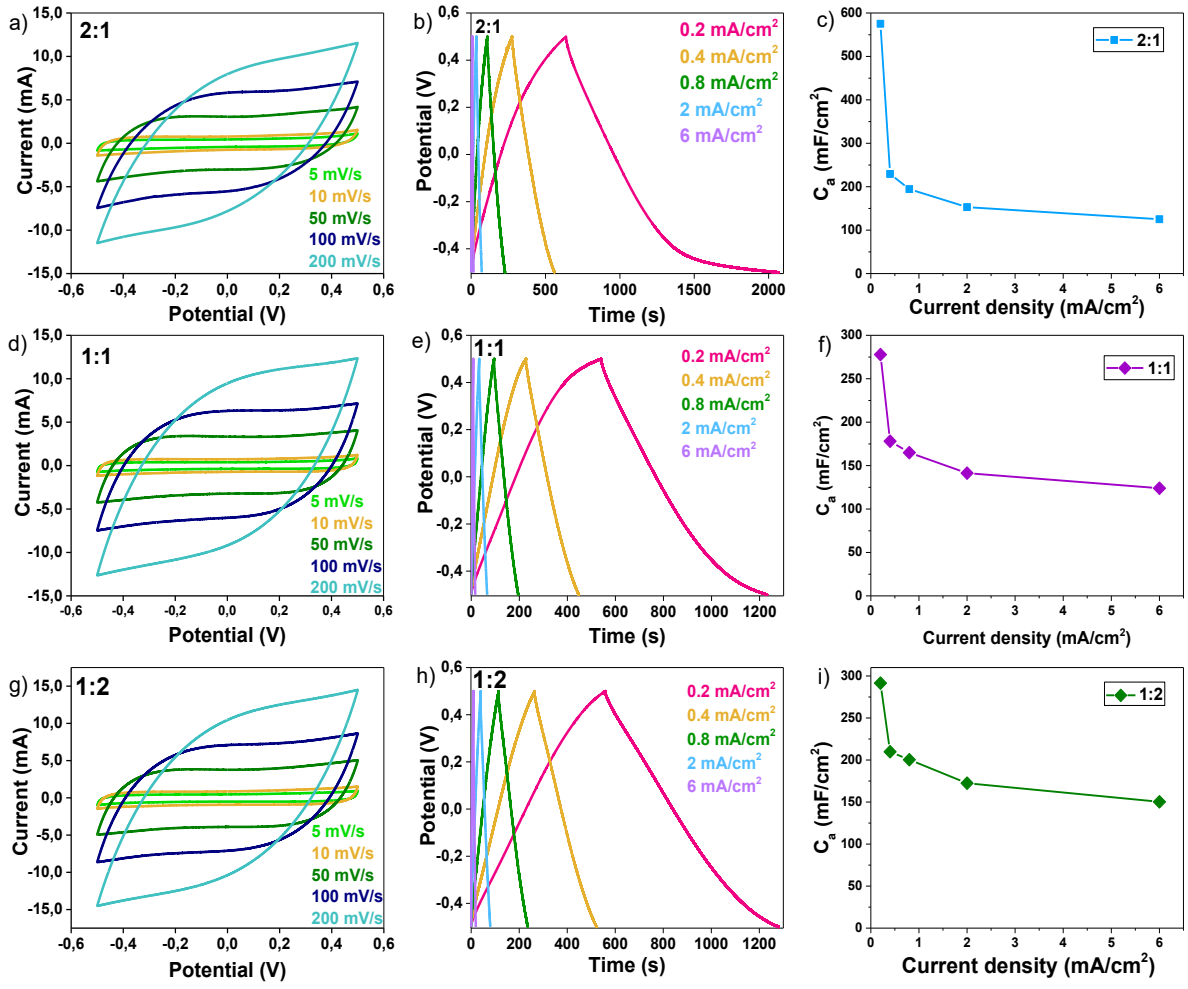

Figure 17 CVs, GCDs and capacitances for samples 2:1, 1:1 and 1:2

Although 1:5 and 1:10 showed decreased interlayer spacing from the intercalation, their electrochemical performance was tested. Results for them are shown in Figure 18. The interlayer spacing didn't increase with 1:5 and 1:10, and neither did capacitance values. C_a was 172 mF/cm^2 and 149 mF/cm^2, respectively, which are significantly lower than for other samples. However, the shapes of the CVs are closer to a rectangular shape. These results correlate with the small interlayer spacing detected in PXRD and with what is reported in literature; lower interlayer spacing results in lower specific capacitance for the material.[31]

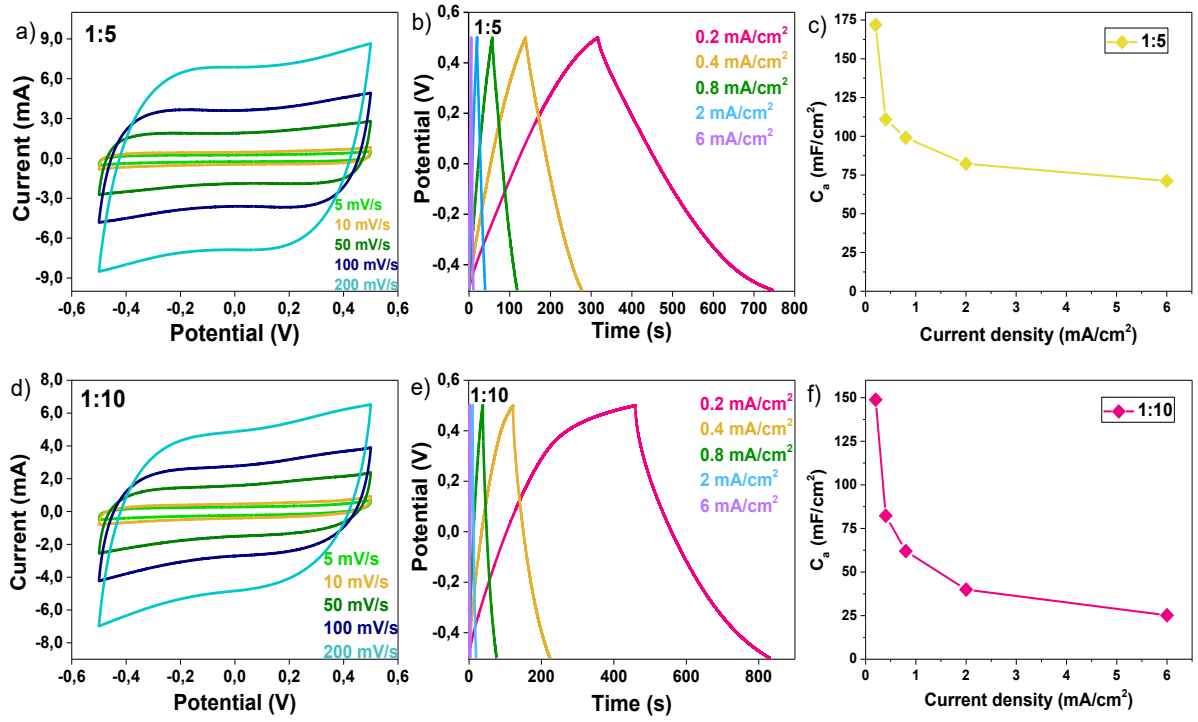

Figure 18 CVs, GCDs and capacitances of 1:5 and 1:10

While the reason for inefficient intercalation with high ratios is unclear, the capacitance might suffer from constant mass loading of active material, which for each electrode was the same, 2 mg/cm^2. As the weight of active material was the same for each electrode, the amount of MXene was less with higher ratios of IL as is seen from TGA. For example, 1:10 electrode had 10 times less MXene than the $Ti_3C_2T_x$ electrode and thus gave lower results as capacitance depends on the active area of the electrode. Accordingly, 2:1 has highest capacitance out of the intercalated samples at 575 mA/cm^2.

Overall, the capacitances obtained for all the intercalated samples are inconsistent showing some variation therefore the experimental errors need to be considered. Getting an even coating

is challenging to achieve consistently, as composition of the mixture consists of different ratios of components that might have affected the measurements.

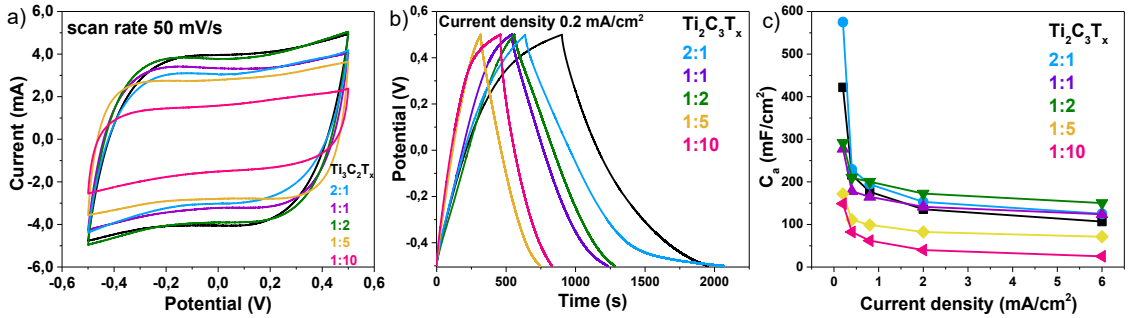

Figure 19 a) CVs of all samples at 50 mV/s, b) comparison of GCD measurements with 0.2 mA/cm^2 current density and c) areal capacitances

In Figure 19a CVs for all the electrodes are shown at scan rate 50 mV/s to compare their performance. 1:10 electrode has significantly lower current compared to other electrodes. 1:2 ratio has the closest performance to $Ti_3C_2T_x$ electrode. In Figure 19b GCDs for the materials are compared at 0.2 mA/cm^2. Figure 19c shows a summary of specific capacitances of each material at all the current densities. While $Ti_3C_2T_x$ has a higher capacitance, capacitance of 2:1 was higher at least at a low current density. Rate performance of the materials is low as specific capacitances decrease by over half as the current density increases. Also, the order of samples with highest performance depends on the current density as is seen in Figure 19c.

Table 3 Capacitance values for MXene and composites obtained from GCD

	C_a (m*F/cm*^{2})
$Ti_3C_2T_x$	422
2:1	575
1:1	277
1:2	291
1:5	172
1:10	149

Stability of the electrodes was studied by performing 10 000 charging – discharging cycles at 10 mA/cm^2. Efficiency and capacitance retention in the electrodes were determined from that data. Despite low specific capacitances, the materials still showed great cycling stability for 10 000 cycles at 10 mA/cm^2, which is typical for MXenes. Figure 20 shows change in efficiency and capacitance over 10 000 cycles for 2:1. The material maintained 97% efficiency and 91 % of its capacitance. Based on these results it's assumed that IL intercalated MXene has overall

good cycling stability but due to challenges with the instrument, timing and the electrochemical cell, the data for all the samples wasn't obtained and thus not included here.

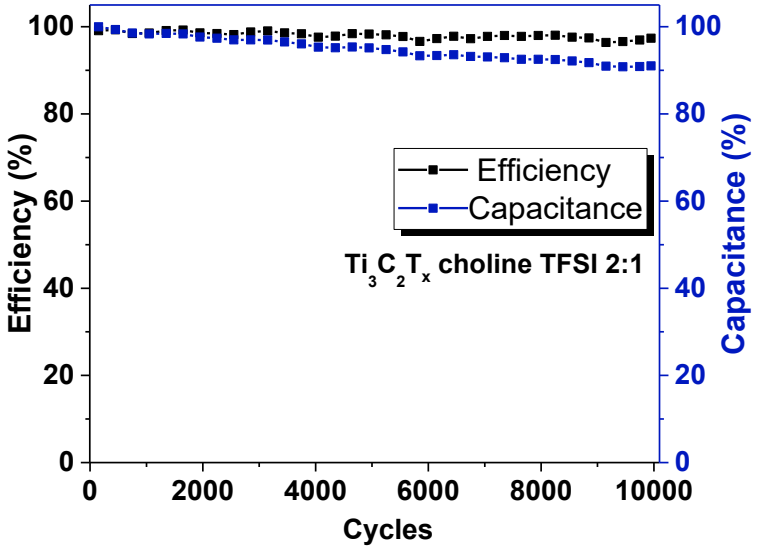

Figure 20 Cycling stability measurement for 2:1 sample

4 Future prospects

This research explores the intercalation of $Ti_3C_2T_x$ with an ionic liquid. It's observed that intercalation of ionic liquid increased the interlayer spacing to some extent with increased MXene:IL ratio, but beyond 2:1, no increase in capacitance is observed. This could be due to changes in surface chemistry as reports have suggested.[25] To get information on this and the intercalation, XPS studies need to be performed on the composite materials. In electrochemical measurements, the mass loading of MXene in composite electrodes should be considered to get better comparable results for the MXene-only electrode. It's also necessary to repeat the experiment with 1 M H_2SO_4 electrolyte, which is the generally used standard concentration.

5 Conclusion

In this work, $Ti_3C_2T_x$ was synthesised via LiF/HCl etching and then intercalated with choline TFSI in five different ratios. Each sample was characterized, and their electrochemical performance was studied with CV and GCD. From the shape of CVs, the capacitive behaviour seems to be EDLC, which could be due to the chosen potential window and the absence of a reference electrode. Based on PXRD, intercalation of choline TFSI into delaminated $Ti_3C_2T_x$ was successful and it had a positive effect on the interlayer spacing in the 2:1, 1:1 and 1:2 samples. 1:2 had higher interlayer spacing than freshly synthesised and vacuum dried $Ti_3C_2T_x$ but 1:5 and 1:10 had the opposite effect.

The conclusion from the electrochemical measurements is that excess intercalation of $Ti_3C_2T_x$ with an ionic liquid doesn't increase the electrochemical performance of the material by giving higher capacitance. Low specific capacitances were due to low concentration of H_2SO_4 electrolyte, but relative performance of the MXene/IL composites was lower than that of $Ti_3C_2T_x$. Only exception was 2:1, which was the lowest ratio used but the higher capacitance than $Ti_3C_2T_x$.

The chosen method of electrode preparation resulted in some lost material and uneven electrode coatings as the outcome of each drop casting was unpredictable, even though the material loss was accounted for in the used amount of material. The quality of electrodes still varied quite a lot in span of the project as the preparation of electrodes was difficult to replicate identically, and it took some time to learn causing inconsistences in the beginning. Quality of the coating seemed to also suffer from absence of conducting carbon. Electrode slurry was made in a mortar, but sonication was another option and might have prevented more drastic material losses.

References

1. Liu, J. *et al.* Advanced Energy Storage Devices: Basic Principles, Analytical Methods, and Rational Materials Design. *Adv. Sci.* **5**, 1700322 (2018).
2. Dunn, B., Kamath, H. & Tarascon, J. M. Electrical energy storage for the grid: A battery of choices. *Science (80-.).* **334**, 928–935 (2011).
3. Emissions by sector - Our World in Data. https://ourworldindata.org/emissions-by-sector.
4. Council on Clean Transportation, I. *Vision 2050: A strategy to decarbonize the global transport sector by mid-century*. (2020).
5. IEA – International Energy Agency. https://www.iea.org/.
6. Zhu, Q., Li, J., Simon, P. & Xu, B. Two-dimensional MXenes for electrochemical capacitor applications: Progress, challenges and perspectives. *Energy Storage Mater.* **35**, 630–660 (2021).
7. Şahin, M. E., Blaabjerg, F. & Sangwongwanich, A. A Comprehensive Review on Supercapacitor Applications and Developments. *Energies* **15**, 674 (2022).
8. Kouchachvili, L., Yaïci, W. & Entchev, E. Hybrid battery/supercapacitor energy storage system for the electric vehicles. *J. Power Sources* **374**, 237–248 (2018).
9. Zhang, L. & Zhao, X. S. Carbon-based materials as supercapacitor electrodes. *Chem. Soc. Rev.* **38**, 2520–2531 (2009).
10. Conway, B. E. *Electrochemical Supercapacitors : Scientific Fundamentals and Technological Applications*. (Springer, 1999).
11. An, C., Zhang, Y., Guo, H. & Wang, Y. Metal oxide-based supercapacitors: progress and prospectives. *Nanoscale Advances* vol. 1 4644–4658 (2019).
12. Naguib, M. *et al.* Two-Dimensional Nanocrystals Produced by Exfoliation of Ti3AlC2. *Adv. Mater.* **23**, 4248–4253 (2011).
13. Anasori, B., Lukatskaya, M. R. & Gogotsi, Y. 2D metal carbides and nitrides (MXenes) for energy storage. *Nat. Rev. Mater.* **2**, 16098 (2017).
14. Mashtalir, O. *et al.* Intercalation and delamination of layered carbides and carbonitrides. *Nat. Commun.* **4**, 1716 (2013).
15. Ghidiu, M., Lukatskaya, M. R., Zhao, M. Q., Gogotsi, Y. & Barsoum, M. W. Conductive two-dimensional titanium carbide 'clay' with high volumetric capacitance. *Nature* **516**, 78–81 (2014).
16. Yang, S. *et al.* Fluoride-Free Synthesis of Two-Dimensional Titanium Carbide (MXene) Using A Binary Aqueous System. *Angew. Chemie* **130**, 15717–15721 (2018).
17. Urbankowski, P. *et al.* Synthesis of two-dimensional titanium nitride Ti_4N_3 (MXene). *Nanoscale* **8**, 11385–11391 (2016).
18. Li, Y. *et al.* A general Lewis acidic etching route for preparing MXenes with enhanced

electrochemical performance in non-aqueous electrolyte. *Nat. Mater.* **19**, 894–899 (2020).

19. Srivastava, P., Mishra, A., Mizuseki, H., Lee, K. R. & Singh, A. K. Mechanistic Insight into the Chemical Exfoliation and Functionalization of Ti_3C_2 MXene. *ACS Appl. Mater. Interfaces* **8**, 24256–24264 (2016).
20. Sokol, M., Natu, V., Kota, S. & Barsoum, M. W. On the Chemical Diversity of the MAX Phases. *Trends in Chemistry* vol. 1 210–223 (2019).
21. Naguib, M. *et al.* Two-Dimensional Transition Metal Carbides. *ACS Nano* **6**, 1322–1331 (2012).
22. Naguib, M., Barsoum, M. W. & Gogotsi, Y. Ten Years of Progress in the Synthesis and Development of MXenes. *Adv. Mater.* **33**, 2103393 (2021).
23. Lukatskaya, M. R. *et al.* Cation Intercalation and High Volumetric Capacitance of Two-Dimensional Titanium Carbide. *Science (80-.).* **341**, 1502–1505 (2013).
24. Tang, Q., Zhou, Z. & Shen, P. Are MXenes Promising Anode Materials for Li Ion Batteries? Computational Studies on Electronic Properties and Li Storage Capability of Ti_3C_2 and $Ti_3C_2X_2$ (X = F, OH) Monolayer. *J. Am. Chem. Soc.* **134**, 16909–16916 (2012).
25. Hart, J. L. *et al.* Control of MXenes' electronic properties through termination and intercalation. *Nat. Commun.* **10**, 522 (2019).
26. Lukatskaya, M. R. *et al.* Probing the Mechanism of High Capacitance in 2D Titanium Carbide Using In Situ X-Ray Absorption Spectroscopy. *Adv. Energy Mater.* **5**, 1500589 (2015).
27. Lin, Z. *et al.* Electrochemical and in-situ X-ray diffraction studies of Ti3C2Tx MXene in ionic liquid electrolyte. *Electrochem. commun.* **72**, 50–53 (2016).
28. Shao, H. *et al.* Unraveling the charge storage mechanism of Ti_3C_2Tx MXene electrode in acidic electrolyte. *ACS Energy Lett.* **5**, 2873–2880 (2020).
29. Okada, Y. *et al.* MXene Electrode Materials for Electrochemical Energy Storage: First-Principles and Grand Canonical Monte Carlo Simulations. *MRS Adv.* **4**, 1833–1841 (2019).
30. Lin, Z. *et al.* Electrochemical and in-situ X-ray diffraction studies of Ti_3C_2Tx MXene in ionic liquid electrolyte. *Electrochem. commun.* **72**, 50–53 (2016).
31. Liang, K. *et al.* Engineering the Interlayer Spacing by Pre-Intercalation for High Performance Supercapacitor MXene Electrodes in Room Temperature Ionic Liquid. *Adv. Funct. Mater.* **31**, 2104007 (2021).
32. Mashtalir, O. *et al.* The effect of hydrazine intercalation on the structure and capacitance of 2D titanium carbide (MXene). *Nanoscale* **8**, 9128–9133 (2016).
33. Carda-Broch, S. & Ruiz-Angel, M. *Ionic Liquids in Analytical Chemistry: New Insights and Recent Developments*. *Ionic Liquids in Analytical Chemistry: New Insights and Recent Developments* (Elsevier, 2021). doi:10.1016/C2019-0-04941-2.
34. Tiago, G. A. O., Matias, I. A. S., Ribeiro, A. P. C. & Martins, L. M. D. R. S. Application of Ionic Liquids in Electrochemistry - Recent Advantaces. *Molecules* **25**, 5812 (2020).

35. Ong, S. P., Andreussi, O., Wu, Y., Marzari, N. & Ceder, G. Electrochemical Windows of Room-Temperature Ionic Liquids from Molecular Dynamics and Density Functional Theory Calculations. *Chem. Mater.* **23**, 2979–2986 (2011).
36. Wang, Z. & Béguin, F. Implementation of a choline bis(trifluoromethylsulfonyl)imide aqueous electrolyte for low temperature EDLCs enabled by a cosolvent. *J. Energy Chem.* **70**, 84–94 (2022).
37. Shekhirev, M., Shuck, C. E., Sarycheva, A. & Gogotsi, Y. Characterization of MXenes at every step, from their precursors to single flakes and assembled films. *Prog. Mater. Sci.* **120**, 100757 (2021).
38. Zou, J. *et al.* Additive-mediated intercalation and surface modification of MXenes. *Chem. Soc. Rev.* **51**, 2972–2990 (2022).
39. Wang, H. *et al.* Surface modified MXene Ti_3C_2 multilayers by aryl diazonium salts leading to large-scale delamination. *Appl. Surf. Sci.* **384**, 287–293 (2016).
40. Ghidiu, M. *et al.* Alkylammonium Cation Intercalation into Ti_3C_2 (MXene): Effects on Properties and Ion-Exchange Capacity Estimation. *Chem. Mater.* **29**, 1099–1106 (2017).
41. Zheng, S. *et al.* Ionic liquid pre-intercalated MXene films for ionogel-based flexible micro-supercapacitors with high volumetric energy density. *J. Mater. Chem. A* **7**, 9478–9485 (2019).
42. Wang, B. *et al.* Carbon dioxide adsorption of two-dimensional carbide MXenes. *J. Adv. Ceram.* **7**, 237–245 (2018).
43. Zhou, H. *et al.* Study on contact angles and surface energy of MXene films. *RSC Adv.* **11**, 5512–5520 (2021).
44. Alhabeb, M. *et al.* Guidelines for Synthesis and Processing of Two-Dimensional Titanium Carbide (Ti_3C_2Tx MXene). *Chem. Mater.* **29**, 7633–7644 (2017).
45. Seredych, M. *et al.* High-Temperature Behavior and Surface Chemistry of Carbide MXenes Studied by Thermal Analysis. *Chem. Mater.* **31**, 3324–3332 (2019).
46. Clough, M. T., Geyer, K., Hunt, P. A., Mertes, J. & Welton, T. Thermal decomposition of carboxylate ionic liquids: trends and mechanisms. *Phys. Chem. Chem. Phys.* **15**, 20480–20495 (2013).
47. Bhattacharyya, S. & Shah, F. U. Thermal stability of choline based amino acid ionic liquids. *J. Mol. Liq.* **266**, 597–602 (2018).
48. Okubo, M., Sugahara, A., Kajiyama, S. & Yamada, A. MXene as a Charge Storage Host. *Acc. Chem. Res.* **51**, 591–599 (2018).
49. Wen, Y. *et al.* Nitrogen-doped Ti_3C_2T x MXene electrodes for high-performance supercapacitors. *Nano Energy* **38**, 368–376 (2017).
50. Lukatskaya, M. R. *et al.* Ultra-high-rate pseudocapacitive energy storage in two-dimensional transition metal carbides. *Nat. Energy* **2**, 1–12 (2017).